



## Magnesium Alloy Anodes for Corrosion Prevention of Reinforcements in Concrete

Yogesh Iyer Murthy<sup>1</sup>, Sumit Gandhi<sup>2</sup> and Abhishek Kumar<sup>3</sup>

<sup>1</sup>Ph. D. Scholar, Department of Civil Engineering,  
Jaypee University of Engineering and Technology, Guna, India.

<sup>2</sup>HOD, Department of Civil Engineering,  
Jaypee University of Engineering and Technology, Guna, India.

<sup>3</sup>Associate Professor, Department of Applied Mechanics,  
Motilal Nehru National Institute of Technology Allahabad, Prayagraj, India.

(Corresponding author: Yogesh Iyer Murthy)

(Received 28 December 2019, Revised 24 February 2020, Accepted 25 February 2020)

(Published by Research Trend, Website: [www.researchtrend.net](http://www.researchtrend.net))

**ABSTRACT:** Corrosion of reinforcements in reinforced cement concrete structures is an active area of research in civil engineering. One of the method of corrosion prevention being cathodic or sacrificial protection. The current work investigates the effect of using pure Mg and AZ91D as sacrificial anodes in ordinary and marine atmosphere on concrete slabs containing partial replacements of cement and fine aggregates by sugar cane bagasse ash (SCBA) and mill scale (MS) respectively by half cell potential (HCP) studies for 270 days. Twelve slabs were casted with centrally placed anodes, tied with the reinforcement cage and HCP readings were observed for 280 days at different locations of the slabs. Slabs were casted without and with 3.5 wt% NaCl. It is observed that at the end of 280 days the slab without any replacement and containing 3.5 wt% NaCl showed maximum values of HCP, whereas, the slabs containing MS or SCBA without any Cl content, showed least HCP values. This is because both MS and SCBA particles, being finer, reduce the porosity of concrete and make it less permeable to chloride ions. It can be concluded that SCBA and MS both act as effective filler materials and behave in similar fashion as far as HCP values are concerned. The micro-structural analysis of AZ91D reveals the formation of cervices due to chipping off of Mg matrix, leading to reduced rate of corrosion compared to pure Mg. It could finally be concluded that the combined effect of using sacrificial protection, alongwith use of alternate materials such as SCBA or MS can further reduce the corrosion of embedded reinforcement.

**Keywords:** AZ91D, filler, Half cell potential, micro-structure, Mill Scale (MS), Sacrificial Anodes, Sugar cane bagasse ash (SCBA).

**Abbreviations:** HCP, half cell potential; MS, Mill Scale; SCBA, Sugar cane bagasse ash.

### I. INTRODUCTION

Reinforced cement concrete (RCC) structures are known for their high strength characteristics. The reinforcement in concrete is expected to provide high tensile and flexural strength to the structure as concrete is weak in tension. But the structural performance of steel depends largely on the exposure conditions. The presence of chlorides, carbonates, sulfates and ionic materials is reported to be detrimental leading to reduced structural performance due to advent of corrosion [1].

Various methods could be found in literature to prevent corrosion of reinforcements. These methods include use of corrosion resistant steel rebars [2], stainless steel and galvanized steel, thermosetting polymers [3], laminates and reinforced plastics [4] thermoplastics, non-metals like elastomers, use of inhibitors [5] paints [6, 7] epoxy coatings [8] powder coating [9] and cathodic protection, each having inherent advantages and disadvantages. The selection of a suitable method would largely depend on the degree of exposure of structure, economics and the discretion of the designer. Among the above-mentioned methods of corrosion prevention, cathodic protection technique is unique as most of the other

methods (except application of corrosion resistant steel rebars and stainless steel and galvanized steel) involve coating of suitable material over the steel and subsequent embedment of steel in concrete. The peeling off of such coatings while pouring of concrete is a common phenomenon resulting in the formation of potential sites for corrosion. On the other hand, cathodic protection involves the installation of suitable electrochemically active electrode as anode as an exterior member, designed for a suitable time period. The application of such anodes as exterior member aids in visual inspection and upon the completion of design period, or otherwise, the anodes can be conveniently replaced. Thus, precise monitoring of reinforcement is enabled. Amongst the commonly used anodes for cathodic protection of steel in concrete are the aluminum, magnesium and zinc anodes, in either pure forms or as alloys at varying proportions.

Among the various commercially available anodes, Mg and its alloy anodes are in major use due to their inherent high electro negative standard potential (i.e. 2.34 V) and high specific charge capacity (2.2 A.h/g) [10] According to literature, Mg anodes shows long term performance of such anodes embedded in concrete.

For example, Parthiban *et.al.* [11] investigated the performance of Mg anode for duration of 42 months on concrete slab made of Ordinary Portland Cement and reported decreased in chloride content with time as the distance from anode decreased from anode confirming the protection of reinforcements. Apostolopoulos and Papadakis [12] studied the mechanism of corrosion initiation, propagation and the subsequent effect of corrosion by exposing steel reinforcements to salt spray atmosphere and investigated the mass loss and mechanical properties of steel. Apostolopoulos *et.al.* [13] did pit depth analysis of reinforcements subjected to chloride induced corrosion using image analysis. One of the significant conclusions drawn from this work was that the steel embedded in concrete and exposed to chloride atmosphere was more vulnerable to pitting corrosion than that exposed directly to chloride atmosphere. Therefore, the reinforcements in concrete are subjected to chloride which creates serious concern for pitting corrosion. The pitting corrosion mechanism is largely influenced by various factors such as the amount of chloride ions, time of exposure, treatment to cover reinforcement and the material properties of cover material, such as permeability and porosity.

Further, in the area of concrete technology for sustainable constructions, there is an increasing trend of replacing cement with low cost materials possessing pozzolanic properties or replacement of fine or coarse aggregates with industrial/agricultural wastes to alleviate the growing demand for the conventional construction materials. Hence, in order to relate the presence of such alternate materials to the corrosion mitigation potential of Mg alloy anodes, there is a pressing demand for systematic investigation. Thus, the aim of the present work is to experimentally investigate the long term effect of addition of agricultural and industrial waste additives in concrete on the half cell potential (HCP) values of reinforced concrete slabs containing pure Mg and AZ91D anodes.

To study the effectiveness of additives in prevention of chloride ingress, sugar cane bagasse ash (SCBA) and mill scale (MS) has been selected as agricultural waste and industrial waste respectively. Experiments were conducted in two sets. First set of experiments consisted of using SCBA as partial replacement of cement because of its pozzolanic activity [14], the mechanical strength gained [15] and durability [16] based advantages of using it in concrete. Another set of experiments were carried out using MS to partially replace fine aggregates of cement due to its inert behavior and to understand its effect on HCP readings; and thereby ascertain the suitability of such concrete in marine atmosphere. Moreover, both the materials, being finer ( $\approx 1 \mu\text{m}$ ) were also expected to act as effective fillers, which would reduce the permeability of free chloride ions towards the reinforcement and hence, expected to be useful in marine atmosphere. Also the partial replacements of the conventional concrete making materials lead to delta contribution towards sustainability and it is an active area for research. For the same, an effort has been made to see the effect of

variations in potential of slabs containing SCBA and MS with slabs containing MS+ free chloride ions and SCBA+ free chloride ions. In this study comparison on the effects of distance from the anode, age of concrete, presence of free chloride ions and microstructure of anodes on the HCP values has also been made. Based on these experimental investigations, conclusions could be drawn relating the selection of anodes for marine atmosphere.

## II. MATERIALS AND METHODS

For the experimentation, SCBA, an agricultural industry waste was collected from Dwarikesh Enterprise, Meerut, India and MS, a metal industry waste was collected from a steel industry, BRD Impex in Pithampur, India. Extensive time taking experiments were designed to obtain optimized values for the replacement of cement with SCBA and fine aggregates with MS based on strength characteristics. One set of experiments were carried out with 5, 10 and 15 wt.% replacements of cement with SCBA and second set of experiments consisted of 10, 20, 30 and 40 wt.% replacement of fine aggregate cement by MS. *Portland Pozzolana* cement was used for casting slabs and coarse aggregates used were 20 mm down, while the fine aggregates conformed grading zone II of Indian Standards IS -383-1970 [17].

Fig. 1 shows the experimental plan used to conduct experiments. Twelve slabs of dimension 1000 mm  $\times$  1000 mm  $\times$  100 mm were casted using 1:1.5:3 nominal mixes and a water to cement ratio of 0.45. 10 mm diameter steel bars were used for making reinforcement mat which were placed with a clear cover of 25 mm from the top and sides with a center to center spacing of 190 mm as shown in Fig. 2. The surface area of steel reinforcement mat was found to be 1.884 m<sup>2</sup>. In order to remove any potential corrosion site, the reinforcements were treated with pickling solution for two hours. Anodes of 22 mm diameter and 250 mm long were carefully placed at the central location as shown in Fig. 2 and tied intact to complete the electrochemical cell. The notations used for all experiments for half-cell potential measurements are presented in Table 1. 3.5 wt.% NaCl by weight of cement was added to concrete while mixing for providing free chloride ions. With rapid interaction of free chloride ions with the ingredients of concrete and formation of HCl, the pH of concrete reduces rapidly. Infiltration of free chloride ions in concrete under marine atmospheres occurs mainly by diffusion through the surface which is in contact with these ions. But this process is very slow and may take many years to be effective. Thus, in order to accelerate the process, NaCl was mixed with the ingredients itself. Also, the mixing of NaCl ensures the availability of sufficient chloride ions for interaction, which results in the exposure of the slab for the extreme environmental condition. All slabs were constructed using tap water with specifications as shown in Table 2 so as to maintain similar casting conditions and all of the slabs were casted in open yard to expose them to the atmosphere.

**Table 1: Nomenclature for different cases of Cathodic protection using pure Mg and AZ91D anodes.**

S.No.	Nomenclature	Expansion of Notation
1.	S10Cl	Slab #1 containing 0% NaCl
2.	S2Cl	Slab #2 containing 3.5 wt.% NaCl of cement
3.	S3MS	Slab #3 containing 0% NaCl and 40 wt.% MS as partial replacement of fine aggregate
4.	S4MSCI	Slab #4 containing 3.5 wt.% NaCl of cement and 40 wt.% MS as partial replacement of fine aggregate
5.	S5SCBA	Slab #5 containing 0% NaCl and 10 wt.% SCBA as partial replacement of cement
6.	S6SCBACI	Slab #6 containing 3.5 wt.% NaCl of cement and 10 wt.% SCBA as partial replacement of cement

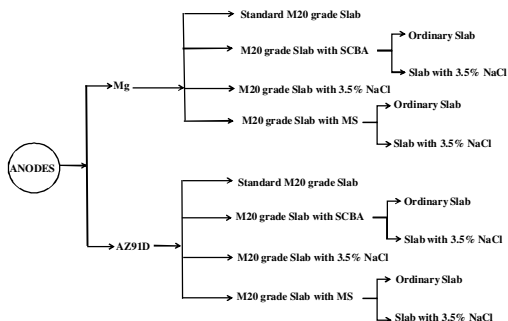


**Fig. 1.** Experimental plan for half-cell potential measurement for cathodic protection using pure Mg and AZ91D anodes.

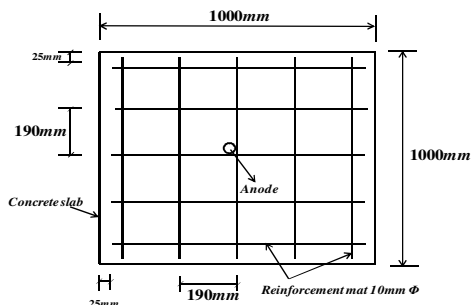


**Fig. 2.** Schematic diagram showing details of reinforcement spacing and position of anodes for all slabs.

**Table 2: Tap water characteristics confirming to IS: 10500:2012 [18].**

S. No.	Parameter	Value
1.	Chloride	162 mg/l
2.	pH	7.6
3.	Fluoride	0.41 mg/l
4.	Dissolved Oxygen	10.25 mg/l
5.	Chemical Oxygen Demand	0
6.	Biological Oxygen Demand	0
7.	Free Residual Chlorine	0.1 mg/l

These are the major factors which influence the corrosion of embedded reinforcements in concrete slabs. The discussion for the experimental investigation is classified into two sections, i.e., the results for pure Mg anode and AZ91D.

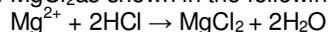
**III. RESULT AND DISCUSSION**

*A. HCP readings for pure Mg anode*

The variation of negative potential of the reinforcements in the slab varying with the distance from the anode is presented in Fig. 3. For standard slab and slab containing 3.5 wt.% NaCl, certain general observations could be made from Fig. 3.

Firstly, the value of electrochemical potential of the slab S2Cl is less dispersed compared to S10Cl, with a major set of value in the range -820 to -610 mV. This implies that for the slab exposed to free chloride ions, the attainment of potential as that of standard slab is a longer process. Secondly, as compared to the standard slab (S10Cl), not much difference is observed with increase in distance from the anode. Thirdly, for both the slabs, the potential values are dispersed at distances 10 cm and 40 cm, that is the nearest to the anode and farthest from anode. This could be attributed to the fact that near the anode (i.e. at 10 cm distance) rapid consumption of chloride ions to form MgCl<sub>2</sub> takes place. This rapid consumption leads to dispersed potential values. Further, towards the end of the slab, i.e. at 40 cm, porosity in the slab is slightly higher compared to the rest of the matrix resulting in higher permeability. Due to this, ingress of free ions from atmosphere is more which could have resulted in dispersed potential values.

It is also observed that as the distance from the anode increases, the negative potential decreases i.e. the potential values obtained at 10 cm from anode are more negative than those at 20 cm from anode. This is because of the fact that the higher electrochemical potential of pure Mg anode renders it as anode and this in turn makes the chloride ions attracted towards the anode. This can also be ascribed to the initiation of radial cracks closer to anode with the increase in number of days. These cracks are formed due to formation of MgCl<sub>2</sub> as shown in the following reaction:



Since, MgCl<sub>2</sub> occupies higher volume compared to pure Mg, cracks are formed near the anodes. It is seen that as the number of days increase, the negative potential decreases for a particular distance from anode because of increasing consumption of chloride and lesser amount of available free chloride.

Further, at a particular distance from anode, the typical difference in potential from the 20<sup>th</sup> day to 280<sup>th</sup> day is approximately 350 mV. During the 220<sup>th</sup> to 280<sup>th</sup> day, the potential at any distance from anode is in the narrow range of -550 to -500mV. Thus, it could be safely concluded that the free chloride is almost fully consumed so that the potential is stabilized at this value. For slabs containing MS, (i.e. S3MS and S4MSCI) and slabs containing SCBA (i.e. S5SCBA and S6SCBACI) similar trends were observed for variation in negative potential. Further, the values ranged with lesser values of maxima and minima compared to the slabs without MS and SCBA. Among the latter two, SCBA had lesser values of negative potential compared to MS. The possible reasons could be smaller particle size and the pozzolanic activity of SCBA due to which it acts as a good filler material and reduces the no of available voids for ingress of free ions.

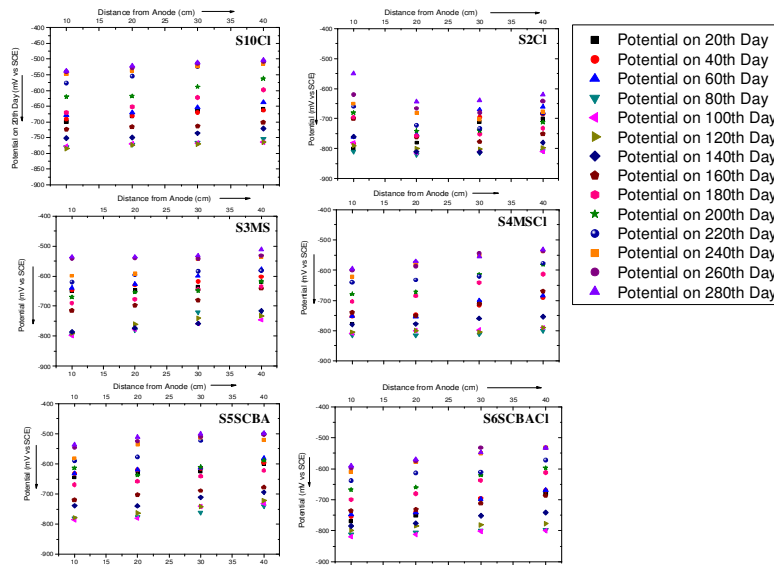


**Fig. 3.** Potential of the embedded reinforcement in mV w.r.t. Standard Calomel Electrode (SCE) with varying proximity from the centrally placed anode on different days for slabs containing pure Mg anode.

**B. HCP readings for AZ91D anode**

The variation of negative potential of the reinforcements in the slab varying with the distance from the anode AZ91D is presented in Fig. 4. In this case, the value of negative electrochemical potential of the slab S10CI is in the range -790 to -525 mV while that of S2CI is in the range -830 to 520 mV. It could be observed from Fig. 4 that at any particular distance from the anode, for all slabs, the extent of dispersion of the HCP values is more in case of AZ91D as compared to pure Mg. For example, for the slab S4MSCI, while the range of values at 30 cm from pure Mg anode was -800 to -540 mV, they range from -780 to -550 mV, from 20<sup>th</sup> day to 280<sup>th</sup>

day. At a particular distance from the anode, the typical difference in potential from the 20<sup>th</sup> to 280<sup>th</sup> day for AZ91D anode is approximately -250 mV. It is also observed that during rainy days i.e. approximately during 120<sup>th</sup> to 180<sup>th</sup> day the most HCP readings fall in the range of -720 to -550mV for S3MS slab. Also, the HCP readings arrive at a nearly stable value nearing -540 mV at approximately 240<sup>th</sup> day. Since MS is inert and fine, it neither reacts with the products of hydration nor permits easy infiltration of free ions. The general range of potential values is towards lesser negative potential compared to standard slab.

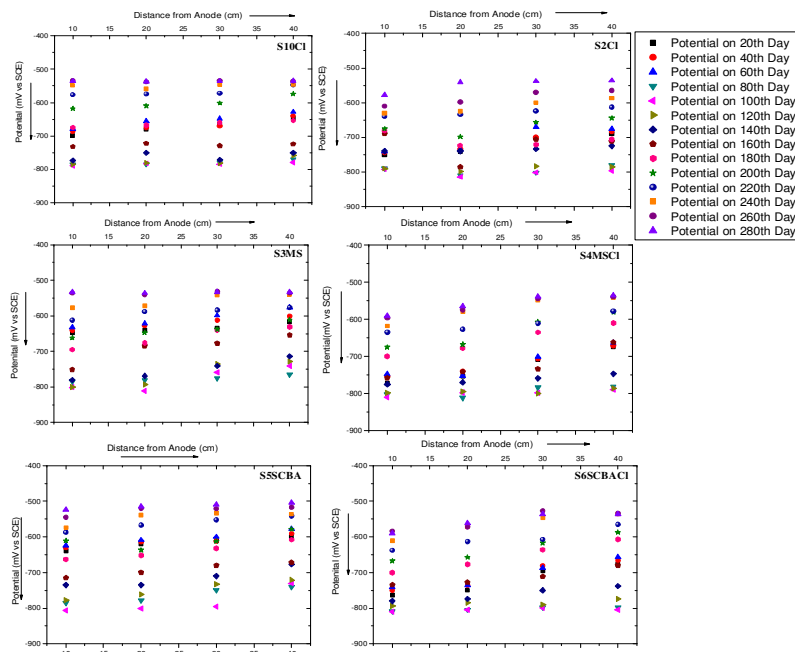


**Fig. 4.** Potential of the embedded reinforcement in mV w.r.t. Standard Calomel Electrode (SCE) with varying proximity from the centrally placed anode on different days for slabs containing AZ91D anode.

### C. Microstructure of Anodes

The microstructure of the embedded anodes, removed from the concrete after 280 days were analyzed using Hitachi S-3400N SEM coupled with Energy Dispersive Spectroscopy (EDS). The analysis of samples was carried out with a 2  $\mu\text{m}$  probe diameter, 10 kV accelerating voltage and 50 nA probe current. The error of the SEM measurements is estimated to be about  $\pm 2$  at %. A comparative study of corroded Mg and AZ91D along with the surface morphology of the un-corroded anodes was done and is presented below.

**(i) Microstructure of pure Mg:** Fig. 5 reveals the backscattered electron images (BSEI) of corroded and un-corroded parts of pure Mg after 280 days of embedment in concrete. Distinct regions could be observed in the micrograph, namely, a matrix of grey with black spots and a matrix which appeared white in color. EDS point analysis was used to understand the composition of these features. The spectral composition of white layer was found to be pure Mg, the grey layer consisted of MgO, while point analysis of the dark grey features confirmed the formation of  $\text{MgCl}_2$  in the corroded region.

Further, Fig. 6 shows the area analysis of 400  $\mu\text{m}$  of corroded part of pure Mg. The area analysis affirms the findings of EDS spot analysis, showing the presence of  $\text{MgCl}_2$  and MgO.

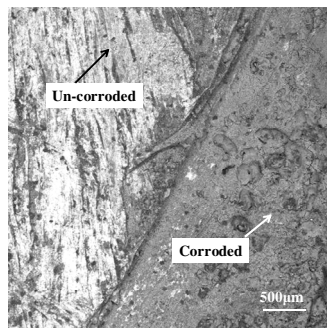


**Fig. 5.** BSEI of corroded and un-corroded parts of pure Mg.

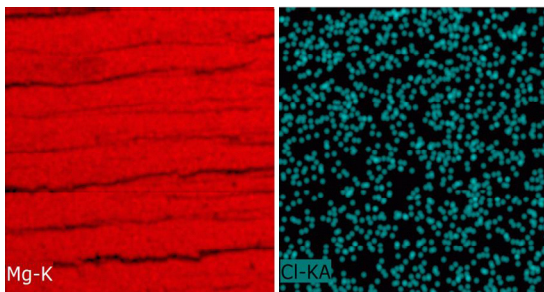


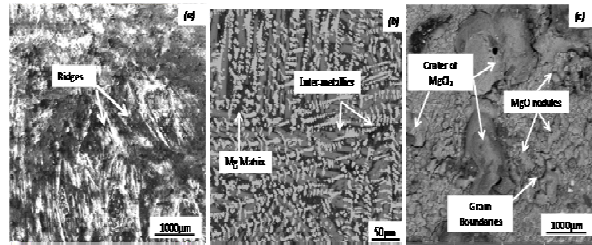
**Fig. 6.** Area analysis of corroded part of pure Mg.

**(ii) Microstructure of AZ91D:** The microstructure of AZ91D was analyzed for the as-cast, un-corroded sample, polished as cast sample and corroded sample removed from the concrete after 280 days. The BSEI of the unpolished as-cast alloy is shown in Fig. 7(a) and consists of ridges. The EDS spot analysis revealed that these ridges were composed of MgO roughly 20  $\mu\text{m}$  long.

Murthy et al., *International Journal on Emerging Technologies* 11(2): 656-661(2020)

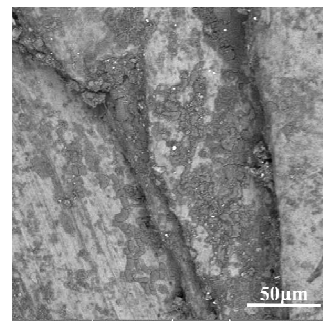
The micro-structure of polished un-corroded as-cast sample of AZ91D is shown in Fig. 7(b). It consists of Mg matrix (Black region) and the inter-metallics consisted of well-developed primary dendrites distributed along the  $\alpha$ -Mg grain boundaries. The inter-metallics consist of  $\text{Mg}_{17}\text{Al}_{12}$  (dark grey) and  $\text{Al}_2\text{Mg}_5\text{Zn}_2$  (light Grey).

Fig. 7(c) shows the BSEI of the corroded AZ91D alloy after 280 days of embedment. It consists of irregular nodules of MgO with varying sizes ranging from 5-40  $\mu\text{m}$  formed due to oxidation of  $\alpha$ -Mg matrix and craters of  $\text{MgCl}_2$  along with the matrix phase. The oxide nodules were formed preferentially at grain boundaries, while craters of  $\text{MgCl}_2$  were randomly distributed.



**Fig. 7.** (a) BSEI of unpolished as-cast AZ91D, (b) BSEI of polished as-cast AZ91D, (c) BSEI of the corroded AZ91D alloy after 280 days of embedment.

A closer examination of some regions of the corroded AZ91D revealed in BSEI (Fig. 8) consists of crevices preferentially along the grain boundaries. It is propounded that the formation of  $\text{MgCl}_2$  and MgO leads to differential expansion of the matrix in comparison to the inter-metallics causing the removal of the former.



**Fig. 8.** BSEI of corroded AZ91D showing crevices.

Further, since the electro-chemical potential of the inter-metallic is lower compared to pure Mg the latter actively interacts with the free ions, while former remains dormant. It is expected that the interactions of inter-metallic with free ions will occur only after the Mg matrix is consumed thereby, lowering the corrosion rate of AZ91D in comparison to pure Mg. Hence, the corrosion process of pure Mg and AZ91D is largely different.

## IV. CONCLUSION

The current work attempts to investigate the long term effects of use of pure Mg and AZ91D on the half-cell potential of concrete slabs containing partial replacements of cement with fine aggregate of MS and SCBA in ordinary and marine atmosphere. Based on this study carried out for 280 days, the following conclusions could be drawn:

–The values of potential on a particular day at all distances from anode follow the order:

S2Cl>S4MSCI>S6SCBACI> S10Cl>S3MS>S5SCBA

It is expected that the slabs containing Cl ions should show higher potential. Since MS and SCBA act as fillers, they reduce the porosity in the slab and hence hinder with the migration of free chloride ions towards anode. Due to this, the potential of slabs S4MSCI and S6SCBACI is less compared to S2Cl. Further, among the former two, the particles of SCBA are finer, which thus acts as a better filler material. Hence the potential of S6SCBACI is lower as compared to S4MSCI. Similar reasons could be used to explain the sequence of potential among the remaining three slabs.

–During monsoon season i.e. from 120<sup>th</sup> to 180<sup>th</sup> day, all the slabs had potential of value nearing -800mV against SCE.

–MS and SCBA both act as effective filler materials and behave in similar fashion as far as HCP values are concerned.

–The micro-structural analysis of pure Mg and AZ91D reveals the formation of cervices due to chipping off of Mg matrix in AZ91D consequently leading to reduced rate of corrosion of AZ91D.

## V. FUTURE SCOPE

Potential dynamic tests on AZ91D anodes can be attempted.

## ACKNOWLEDGEMENTS

The authors wish to thank to the faculties and staff of Department of Civil Engineering at Jaypee University of Engineering and Technology, Guna for the technical support.

**Conflict of Interest.** The authors declare no conflict of interest associated with this work.

## REFERENCES

- [1]. Neville, A. M. (1995). *Properties of concrete* (Vol. 4). London: Longman.
- [2]. Hurley, M. F., and Scully, J. R. (2006). Threshold chloride concentrations of selected corrosion-resistant rebar materials compared to carbon steel. *Corrosion*, 62(10), 892-904.
- [3]. Sun, H., Wei, L., Zhu, M., Han, N., Zhu, J. H., & Xing, F. (2016). Corrosion behavior of carbon fiber reinforced polymer anode in simulated impressed current cathodic protection system with 3% NaCl solution. *Construction and Building Materials*, 112, 538-546.
- [4]. Yeh, J. M., & Chang, K. C. (2008). Polymer/layered silicate nanocomposite anticorrosive coatings. *Journal of Industrial and Engineering Chemistry*, 14(3), 275-291.

- [5]. Gaidis, J. M. (2004). Chemistry of corrosion inhibitors. *Cement and Concrete Composites*, 26(3), 181-189.

- [6]. Mayne, J. E. O. (1970). Paints for the protection of steel—A review of research into their modes of action. *British Corrosion Journal*, 5(3), 106-111.

- [7]. Das, S. C., Pouya, H. S., & Ganjian, E. (2015). Zinc-rich paint as anode for cathodic protection of steel in concrete. *Journal of Materials in Civil Engineering*, 27(11).

- [8]. Saravanan, K., Sathiyarayanan, S., Muralidharan, S., Azim, S. S., & Venkatachari, G. (2007). Performance evaluation of polyaniline pigmented epoxy coating for corrosion protection of steel in concrete environment. *Progress in Organic Coatings*, 59(2), 160-167.

- [9]. Di, H., Yu, Z., Ma, Y., Zhang, C., Li, F., Lv, L., & He, Y. (2016). Corrosion-resistant hybrid coatings based on graphene oxide–zirconia dioxide/epoxy system. *Journal of the Taiwan Institute of Chemical Engineers*, 67, 511-520.

- [10]. Jia, X., Yang, Y., Wang, C., Zhao, C., Vijayaraghavan, R., MacFarlane, D. R., & Wallace, G. G. (2014). Biocompatible ionic liquid–biopolymer electrolyte-enabled thin and compact magnesium–air batteries. *ACS applied materials & interfaces*, 6(23), 21110-21117.

- [11]. Parthiban, G. T., Parthiban, T., Ravi, R., Saraswathy, V., Palaniswamy, N., & Sivan, V. (2008). Cathodic protection of steel in concrete using magnesium alloy anode. *Corrosion Science*, 50(12), 3329-3335.

- [12]. Apostolopoulos, C. A., & Papadakis, V. G. (2008). Consequences of steel corrosion on the ductility properties of reinforcement bar. *Construction and Building Materials*, 22(12), 2316-2324.

- [13]. Apostolopoulos, C. A., Demis, S., & Papadakis, V. G. (2013). Chloride-induced corrosion of steel reinforcement—Mechanical performance and pit depth analysis. *Construction and Building Materials*, 38, 139-146.

- [14]. Berenguer, R. A., Helene, P., Silva, F. A. N., Torres, S. M., Monteiro, E. C. B., & de Melo Neto, A. A. (2018). On the influence of sugarcane bagasse ashes as a partial replacement of cement in compressive strength of mortars. *Revista ALCONPAT*, 8(1), 30-37.

- [15]. Shafiq, N., Hussein, A. A. E., Nuruddin, M. F., & Al Mattarneh, H. (2016). Effects of sugarcane bagasse ash on the properties of concrete. *Proceedings of the Institution of Civil Engineers-Engineering Sustainability*, 171(3), 123-132.

- [16]. Pereira, A., Akasaki, J. L., Melges, J. L., Tashima, M. M., Soriano, L., Borrachero, M. V., & Payá, J. (2015). Mechanical and durability properties of alkali-activated mortar based on sugarcane bagasse ash and blast furnace slag. *Ceramics International*, 41(10), 13012-13024.

- [17]. IS: 383. (1970) Specification for coarse and fine aggregates from natural sources for concrete.

- [18]. IS: 10500 (1991). Specification for drinking water.

**How to cite this article:** Murthy, Y. I., Gandhi, S. and Kumar, A. (2020). Magnesium Alloy Anodes for Corrosion Prevention of Reinforcements in Concrete. *International Journal on Emerging Technologies*, 11(2): 656–661.